

Explosive lithium production in the classical nova V339 Del (Nova Delphini 2013)

Akito Tajitsu¹, Kozo Sadakane², Hiroyuki Naito^{3,4}, Akira Arai^{5,6} & Wako Aoki⁷

¹*Subaru Telescope, National Astronomical Observatory of Japan, 650 North A'ohoku Place, Hilo, HI 96720, USA*

²*Astronomical Institute, Osaka Kyoiku University, Asahigaoka, Kashiwara, Osaka 582-8582, Japan*

³*Graduate School of Science, Nagoya University, Furo-cho, Chikusa-ku, Nagoya 464-8602, Japan*

⁴*Nayoro Observatory, 157-1 Nisshin, Nayoro, Hokkaido 096-0066, Japan*

⁵*Center for Astronomy, University of Hyogo, Sayo-cho, Hyogo 679-5313, Japan*

⁶*Koyama Astronomical Observatory, Kyoto Sangyo University, Motoyama, Kamigamo, Kita-ku, Kyoto 603-8555, Japan*

⁷*National Astronomical Observatory of Japan, 2-21-1 Osawa, Mitaka, Tokyo 181-8588, Japan*

The origin of lithium (Li) and its production process have long been an unsettled question in cosmology and astrophysics. Candidates environments of Li production events or sites suggested by previous studies include big bang nucleosynthesis, interactions of energetic cosmic rays with interstellar matter, evolved low mass stars, novae, and supernova explosions. Chemical evolution models and observed stellar Li abundances suggest that at least half of the present Li abundance may have been produced in red giants, asymptotic giant branch (AGB) stars, and novae¹⁻³. However, no direct evidence for the supply of Li from stellar ob-

jects to the Galactic medium has yet been found. Here we report on the detection of highly blue-shifted resonance lines of the singly ionized radioactive isotope of beryllium, ${}^7\text{Be}$, in the near ultraviolet (UV) spectra of the classical nova V339 Del (Nova Delphini 2013). Spectra were obtained 38 to 48 days after the explosion. ${}^7\text{Be}$ decays to form ${}^7\text{Li}$ within a short time (half-life 53.22 days⁴). The spectroscopic detection of this fragile isotope implies that it has been created during the nova explosion via the reaction ${}^3\text{He}(\alpha, \gamma){}^7\text{Be}$ (ref. 5), and supports the theoretical prediction that a significant amount of ${}^7\text{Li}$ could be produced in classical nova explosions. This finding opens a new way to explore ${}^7\text{Li}$ production in classical novae and provides a clue to the mystery of the Galactic evolution of lithium.

V339 Del (= Nova Delphini 2013) is a classical nova that was discovered as a bright 6.8 magnitude (unfiltered) source on 2013 August 14.584 Universal Time (UT)⁶. After 40 hours from the discovery, a maximum was reached on Aug 16.25 (MJD = 56,520.25) at $V = 4.3$ (ref. 7). Then, it began a normal decline.

High-resolution spectra ($R = 90,000\text{--}60,000$) of V339 Del were obtained at four epochs after its outburst (+38, +47, +48, and +52 d). These spectra contain a series of broad emission lines originating from neutral hydrogen (H I, Balmer series) and other permitted transitions of neutral or singly ionized species (e.g., Fe II, He I, Ca II). These emission lines are usually seen in post-outburst spectra of classical novae. Most of these broad emission lines are accompanied by sharp and blue-shifted multiple absorption lines at their blue edges. The typical radial velocity (v_{rad}) of these highly blue-shifted absorption lines is $\sim -1,000 \text{ km s}^{-1}$. Figure 1-a and -b display

the spectrum obtained at +47 d in the vicinities of H η and Ca II K lines, respectively. The H I line is accompanied by a broad emission with a FWHM of $\sim 1,300 \text{ km s}^{-1}$ centered at $v_{\text{rad}} \sim 0 \text{ km s}^{-1}$. The Ca II K (and H) has a weak but broad emission and strong absorption components caused by the interstellar (IS) absorptions. In addition to these profiles around the rest positions of both lines, two sharp absorption components are found at $v_{\text{rad}} = -1,268 \pm 2$ and $-1,103 \pm 1 \text{ km s}^{-1}$. Among these, the latter is apparently stronger than the former. Such absorption line systems have been found in post-outburst spectra of several classical novae^{8,9}. The absorption line systems in V339 Del contain numerous transitions originating from singly ionized iron-group species (Fe II, Ti II, Cr II, Mn II, and Ni II). The depths of all blue-shifted absorption lines in V339 Del are only $\lesssim 25\%$ of the continuum, while the bottoms of some strong lines (e.g., Balmer lines; see Extended Data Fig. 2) have flat features suggesting that the absorption is saturated. These observational results can be interpreted as the effect of absorbing materials partially covering the background light source. There are no Na I D doublet lines, which are often found to be the strongest absorption features in novae within a few weeks after their outbursts^{8,10}. We interpret this as indicating that the ionization state of the ejected gas has evolved into a higher stage of excitation before our observing epochs (5–7 weeks). The observed spectral energy distribution of this nova indicates that the shape of the continuous radiation had entered a very hot stage (effective temperature $> 100,000 \text{ K}$) within 5 weeks after the explosion¹¹. Other observed characteristics of this nova (e.g., light curves, optical and UV emission lines) show that it is a typical Fe II nova with a CO white dwarf (WD)^{12,13}.

Among these absorption line systems, we have noticed two remarkable pairs of absorption features near 312 nm. These correspond to the absorption components originating from transitions

at ~ 313 nm. These pairs are marked as A, B and C, D, respectively, in Figure 1-c. Adopting the wavelengths of the resonance doublet lines of singly ionized ${}^7\text{Be}$ at 313.0583 and 313.1228 nm^{14,15}, we find that features A and B coincide with the $-1,103 \text{ km s}^{-1}$ components of the 313.0583 and 313.1228 nm lines, respectively. Similarly, features C and D coincide with the $-1,268 \text{ km s}^{-1}$ components of these two lines. Separations in wavelength between features A and B, and between features C and D are consistent with the separation between the doublet lines within the measurement uncertainties. Figure 1-d illustrates these coincidences on the velocity scale. Thanks to the high resolution of the spectrum (~ 0.0052 nm), we can clearly distinguish them from the doublet of ${}^9\text{Be}$ II at 313.0422 and 313.1067 nm¹⁴. After ruling out the possibilities of alternative identifications, we conclude that these absorption features at 312 nm are caused by ${}^7\text{Be}$, and not by ${}^9\text{Be}$ which is the only stable isotope of Be. Original ${}^9\text{Be}$ contained in the progenitor star would have been depleted during its evolution because this isotope is destroyed at temperatures $T > 3 \times 10^6$ K. On the other hand, production of the unstable isotope ${}^7\text{Be}$ by the reaction ${}^3\text{He}(\alpha, \gamma){}^7\text{Be}$ in nova explosions has been theoretically predicted^{16–21}.

The transition probability of the ${}^7\text{Be}$ II line at 313.0583 nm ($\log gf = -0.178$) is twice as large as that of the ${}^7\text{Be}$ II at 313.1228 nm ($\log gf = -0.479$)¹⁴. Due to saturation effects, the ratio of their equivalent widths is expected to be in the range between 2 (no saturation) to 1 (complete saturation). The measured ratios are 1.1 ± 0.3 and 1.6 ± 0.4 for the components at $v_{\text{rad}} = -1,268$ and $-1,103 \text{ km s}^{-1}$, respectively. These are within the range expected for the doublet, although the values contain some errors ($\lesssim \pm 25\%$) due mainly to the uncertainty in the continuum placement. The weaker component at $v_{\text{rad}} = -1,268 \text{ km s}^{-1}$ has a ratio closer to complete saturation. This can

be interpreted as resulting from the fact that the absorbing gas cloud moving with $v_{\text{rad}} = -1,268$ km s⁻¹ has a smaller covering factor, and at the same time, higher column density of ⁷Be ion than the gas cloud moving with $v_{\text{rad}} = -1,103$ km s⁻¹.

Figure 2 displays the velocity plots of normalized spectra for different species of the absorption line systems at four observing epochs from +38 to +52 d. On +38 d, the ⁷Be II doublet has an absorption component at $v_{\text{rad}} = -1,386 \pm 3$ km s⁻¹ and shows a complicated profile near $v_{\text{rad}} \sim -1,000$ km s⁻¹. From +47 to +48 d, the absorption components at $v_{\text{rad}} = -1,268$ and $-1,103$ km s⁻¹ in +47 d shift by -26 ± 3 and -17 ± 4 km s⁻¹ blueward, respectively. These changes can be interpreted as due to the fact that we are observing accelerating blobs of nova ejecta. All of the blue-shifted absorption line systems had disappeared in the spectrum of +52 d except for the meta-stable He I lines at 318.8 and 388.9 nm. This fact indicates that the gas in the absorption line systems have evolved into a higher ionization stage as discussed in the case of the nova V1280 Sco²². These observations show – (1) Several blue-shifted absorption lines with different velocities are found from different species at each epoch; (2) Radial velocities of different transitions belonging to a velocity component determined by Gaussian fittings agree within $|\Delta v_{\text{rad}}| < 1-3$ km s⁻¹; (3) Each component shifts blueward with time, indicating that the ejecta is being accelerated; (4) The strengths of the blue-shifted absorption lines weaken quickly during the observing period. The velocities and the strengths of the ⁷Be II doublet behave perfectly synchronized with those of other species. This means that the gas producing the absorption line systems of V339 Del contains a considerable amount of ⁷Be ion which can produce detectable absorption lines and strongly suggests that the gas must have experienced an explosive thermonuclear runaway on

the surface of the WD.

Our spectroscopic detection of ${}^7\text{Be}$ in a classical nova immediately connects to the production of ${}^7\text{Li}$. The production of ${}^7\text{Be}$ via the nuclear reaction ${}^3\text{He}(\alpha, \gamma){}^7\text{Be}$ in novae has been studied theoretically. However, no observational confirmation has been made up to the present time. This is because the presence of ${}^7\text{Be}$ is very transient and is only observable in the near UV range where the atmospheric absorption severely obstructs observations from ground-based telescopes. In the case of V339 Del, the ${}^7\text{Be}$ doublet can be identified only within a very short period (from ~ 6 to ~ 7 weeks after the outburst). In earlier epochs, it might be difficult to identify due to saturation effects. For nearby bright novae, there have been several attempts to detect the 478 keV gamma-ray line produced by the decay of ${}^7\text{Be}$. However, no definite detection has been reported because of the insufficient sensitivity^{23,24}. The ${}^7\text{Be}$ absorption lines in the near UV spectrum of V339 Del are found in highly blue-shifted ($\sim 1,000 \text{ km s}^{-1}$) flows, which have been blown off by the outburst. This means that it will soon decay to ${}^7\text{Li}$ in cooler interstellar or circumstellar matter on a time scale given by the half-life of ${}^7\text{Be}$ (53.22 days). The absence of the ${}^7\text{Li I}$ line at 670.8 nm in our spectra can be interpreted as due to the fact that all of Li in the absorbing material of V339 Del has been ionized during the observing period as mentioned above. This is in accordance with the fact that no Na I D lines are found in the absorption line system.

The ${}^7\text{Be II}$ doublet corresponds to the doublet of the Ca II resonance lines (H and K lines) on the atomic energy level diagrams. The Ca II K line at 393.366 nm has $\log gf = +0.135$ (ref. 14). Supposing that most of the ${}^7\text{Be}$ and Ca in the absorption line system are singly ionized and the

resonance lines of both ions are unsaturated, the ratio of their equivalent widths directly reflects the number density ratio between ${}^7\text{Be}$ and Ca ions. In the spectrum obtained at +47 d, the ratios of ${}^7\text{Be II}$ (313.1228 nm)/Ca II K, which are less affected by saturation and/or contamination, are $\sim 1.3 \pm 0.3$ and $\sim 0.7 \pm 0.2$ for the $-1,268$ and the $-1,103 \text{ km s}^{-1}$ components, respectively. This means that the column number density of ${}^7\text{Be}$ is 5.3–2.9 times higher than that of Ca. Using this ${}^7\text{Be}/\text{Ca}$ number ratio, the mass fraction of ${}^7\text{Be}$ relative to the sum of all the constituent mass components, $X({}^7\text{Be})$, is presented as $(4.4 \pm 2.2) \times 7/40 \times X(\text{Ca})$. If we adopt the solar $X(\text{Ca})$ ($= 10^{-4.19}$), for instance, the $X({}^7\text{Be})$ in the absorbing gas system should amount to $\sim 10^{-4.3 \pm 0.3}$. The error estimation includes the uncertainty in the local continuum placement ($\lesssim \pm 25\%$) and the difference of derived equivalent widths derived from individual velocity components ($\sim \pm 30\%$). Several additional factors, such as the abundance of Ca in the absorbing gas, and the difference in the ionization state between ${}^7\text{Be}$ and Ca, are difficult to estimate because the nova ejecta model is not yet established. Taking such uncertainties into account, the error involved in the above estimate of the ${}^7\text{Be}$ abundance could be even larger by a factor of several. However, in spite of the large uncertainty, the abundance of ${}^7\text{Be}$ is larger than, or at least as large as, theoretical predictions for CO novae [e.g., $X({}^7\text{Be}) \lesssim 10^{-5.1}$ (ref. 21)]. This indicates that classical novae could play an important role as contributors of ${}^7\text{Li}$ in the Galaxy.

The observed ${}^7\text{Li}$ evolutionary curve³ has a plateau for young Galactic ages ($\lesssim 2.5$ Gyr) followed by a steep rise. To explain this requires a relatively low-mass stellar component that evolves over a long lifetimes. Candidates for this, such as low-mass red giants or novae, have been proposed to be major sources of ${}^7\text{Li}$ production ($> 50\%$ of the solar system Li measured

in meteorites) in the Galaxy^{1–3}. The production of ${}^7\text{Li}$ in low-mass stars has been theoretically studied^{25–29}, and Li-enhanced red giants and AGB stars are indeed identified³⁰. The contribution to Li enrichment in the Galaxy by these objects has, however, not been confirmed. The reason for this is that the Li-rich phase in these stars might be of quite limited duration and the contribution is dependent upon the mass-loss rate of such objects. Nova eruptions involve a long delay time before working as stellar ${}^7\text{Li}$ factories. This is because ${}^3\text{He}$ rich low mass secondaries are necessary to produce ${}^7\text{Be}$ efficiently via the ${}^3\text{He}(\alpha, \gamma){}^7\text{Be}$ reaction¹⁸. It is important to know whether this phenomenon is common among classical novae to quantify their contribution to the rapid increase of ${}^7\text{Li}$ in the Galaxy. Since V339 Del appears to be one of the ordinary Fe II type novae which occupy $\sim 60\%$ of all classical novae¹², the ${}^7\text{Be}$ production found in this object might be occurring in many classical novae. Our successful detection of ${}^7\text{Be}$ in V339 Del indicates that measurements of the ${}^7\text{Be}$ lines in the near UV range for post-outburst novae within the lifetime of this isotope is a powerful way to estimate the contribution of novae to the chemical evolution of lithium in the Galaxy.

1. Romano, D., Matteucci, F., Molaro, P. & Bonifacio, P. The galactic lithium evolution revisited. *Astron. Astrophys.* **352**, 117–128 (1999).
2. Romano, D., Matteucci, F., Ventura, P. & D’Antona, F. The stellar origin of ${}^7\text{Li}$. Do AGB stars contribute a substantial fraction of the local Galactic lithium abundance? *Astron. Astrophys.* **374**, 646–655 (2001).
3. Prantzos, N. Production and evolution of Li, Be, and B isotopes in the Galaxy.

- Astron. Astrophys.* **542**, A67 (2012).
4. Audi, G., Bersillon, O., Blachot, J. & Wapstra, A. H. The NUBASE evaluation of nuclear and decay properties. *Nucl. Phys. A* **729**, 3–128 (2003).
 5. Cameron, A. G. W. & Fowler, W. A. Lithium and the s-PROCESS in Red-Giant Stars. *Astrophys. J.* **164**, 111–114 (1971).
 6. Waagen, E. O. Nova Delphini 2013 = PNV J20233073+2046041. *AAVSO Alert Notice* **489** (2013).
 7. Munari, U. *et al.* After a post-maximum plateau Nova Del 2013 has begun a normal decline. *Astron. Telegr.* **5304**, 1 (2013).
 8. Williams, R., Mason, E., Della Valle, M. & Ederoclite, A. Transient Heavy Element Absorption Systems in Novae: Episodic Mass Ejection from the Secondary Star. *Astrophys. J.* **685**, 451–462 (2008).
 9. Sadakane, K., Tajitsu, A., Mizoguchi, S., Arai, A. & Naito, H. Discovery of Multiple High-Velocity Narrow Circumstellar NaI D Lines in Nova V1280 Sco. *Publ. Astron. Soc. Jpn* **62**, L5–L10 (2010).
 10. McLaughlin, D. B. The Spectra of Novae. In Greenstein, J. L. (ed.) *Stellar Atmospheres*, 585–652 (The University of Chicago Press, 1960).
 11. Skopal, A. *et al.* Early evolution of the extraordinary Nova Delphini 2013 (V339 Del). *Astron. Astrophys.* **569**, A112 (2014).

12. Williams, R. E. The formation of novae spectra. *Astron. J.* **104**, 725–733 (1992).
13. Warner, B. Cataclysmic variable stars. *Cambridge Astrophysics Series* **28**, 257–306 (1995).
14. Kramida, A., Yu. Ralchenko, Reader, J. & and NIST ASD Team. NIST Atomic Spectra Database (ver. 5.1), [Online]. Available: <http://physics.nist.gov/asd> [2014, June 26]. National Institute of Standards and Technology, Gaithersburg, MD. (2013).
15. Yan, Z.-C., Nörtershäuser, W. & Drake, G. W. F. High Precision Atomic Theory for Li and Be⁺: QED Shifts and Isotope Shifts. *Phys. Rev. Lett.* **100**, 243002 (2008).
16. Arnould, M. & Norgaard, H. The Explosive Thermonuclear Formation of ⁷Li and ¹¹B. *Astron. Astrophys.* **42**, 55–70 (1975).
17. Starrfield, S., Truran, J. W., Sparks, W. M. & Arnould, M. On Li-7 production in nova explosions. *Astrophys. J.* **222**, 600–603 (1978).
18. D’Antona, F. & Matteucci, F. Galactic evolution of lithium. *Astron. Astrophys.* **248**, 62–71 (1991).
19. Boffin, H. M. J., Paulus, G., Arnould, M. & Mowlavi, N. The explosive thermonuclear formation of Li-7 revisited. *Astron. Astrophys.* **279**, 173–178 (1993).
20. Hernanz, M., Jose, J., Coc, A. & Isern, J. On the Synthesis of ⁷Li and ⁷Be in Novae. *Astrophys. J.* **465**, L27–L30 (1996).
21. José, J. & Hernanz, M. Nucleosynthesis in Classical Novae: CO versus ONe White Dwarfs. *Astrophys. J.* **494**, 680–690 (1998).

22. Naito, H., Tajitsu, A., Arai, A. & Sadakane, K. Discovery of Metastable Helium Absorption Lines in V1280 Scorpii. *Publ. Astron. Soc. Jpn* **65**, 37 (2013).
23. Harris, M. J. *et al.* Transient Gamma-Ray Spectrometer Observations of Gamma-Ray Lines from Novae. III. The 478 keV Line from ${}^7\text{Be}$ Decay. *Astrophys. J.* **563**, 950–957 (2001).
24. Hernanz, M. Gamma-rays from Classical Novae. In Bode, M. F. & Evans, A. (eds.) *Classical Novae, 2nd Edition. Cambridge Astrophysics Series, No. 43*, 252–284 (Cambridge University Press, 2008).
25. Sackmann, I.-J. & Boothroyd, A. I. Creation of ${}^7\text{Li}$ and Destruction of ${}^3\text{He}$, ${}^9\text{Be}$, ${}^{10}\text{B}$, and ${}^{11}\text{B}$ in Low-Mass Red Giants, Due to Deep Circulation. *Astrophys. J.* **510**, 217–231 (1999).
26. de la Reza, R., da Silva, L., Drake, N. A. & Terra, M. A. On ${}^7\text{Li}$ Enrichment by Low-Mass Metal-Poor Red Giant Branch Stars. *Astrophys. J.* **535**, L115–L117 (2000).
27. Sackmann, I.-J. & Boothroyd, A. I. The creation of super-rich lithium giants. *Astrophys. J.* **392**, L71–L74 (1992).
28. Travaglio, C. *et al.* Galactic Chemical Evolution of Lithium: Interplay between Stellar Sources. *Astrophys. J.* **559**, 909–924 (2001).
29. Ventura, P. & D’Antona, F. The role of lithium production in massive AGB and super-AGB stars for the understanding of multiple populations in globular clusters. *Mon. Not. R. Astron. Soc.* **402**, L72–L76 (2010).

30. Melo, C. H. F. *et al.* On the nature of lithium-rich giant stars. Constraints from beryllium abundances. *Astron. Astrophys.* **439**, 227–235 (2005).

Acknowledgements This work is based on data collected at Subaru Telescope, which is operated by the National Astronomical Observatory of Japan (NAOJ). We acknowledge with thanks the variable star observations from the AAVSO International Database contributed by observers worldwide and used in this research.

Author Contribution A.T. planned and carried out Subaru HDS observations, reduced and analyzed the data and prepared the manuscript. K.S., H.N., A.A., and W.A. participated in the discussion and contributed in the process of manuscript preparation significantly.

Competing Interests The authors declare that they have no competing financial interests.

Correspondence Correspondence and requests for materials should be addressed to A.T. (email: tajitsu@naoj.org).

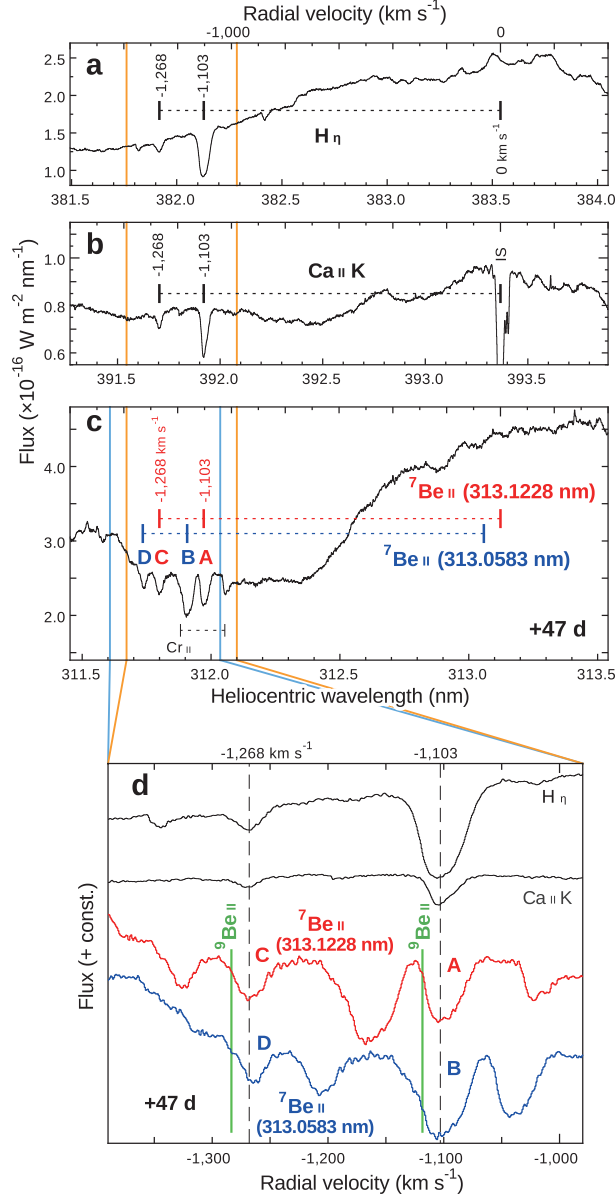


Figure 1: **Blue-shifted absorption line systems in the spectrum of V339 Del obtained at +47 day.** Panels a–c display the spectrum in the vicinity of $H\eta$ (a), Ca II K (b), and the ${}^7\text{Be II}$ doublet (c), on the velocity (upper horizontal) scale. Two blue-shifted absorption components and the zero velocity position for each line are indicated by ticks. c, The velocity scale is adjusted to one of the ${}^7\text{Be II}$ doublet (313.1228 nm, red). The positions of blue-shifted components of Cr II at 313.205 nm are displayed at the bottom. Panel d shows the enlarged radial velocity profiles. The vertical dashed lines show two common absorption components. The expected positions of the ${}^9\text{Be II}$ doublet are indicated by green lines.

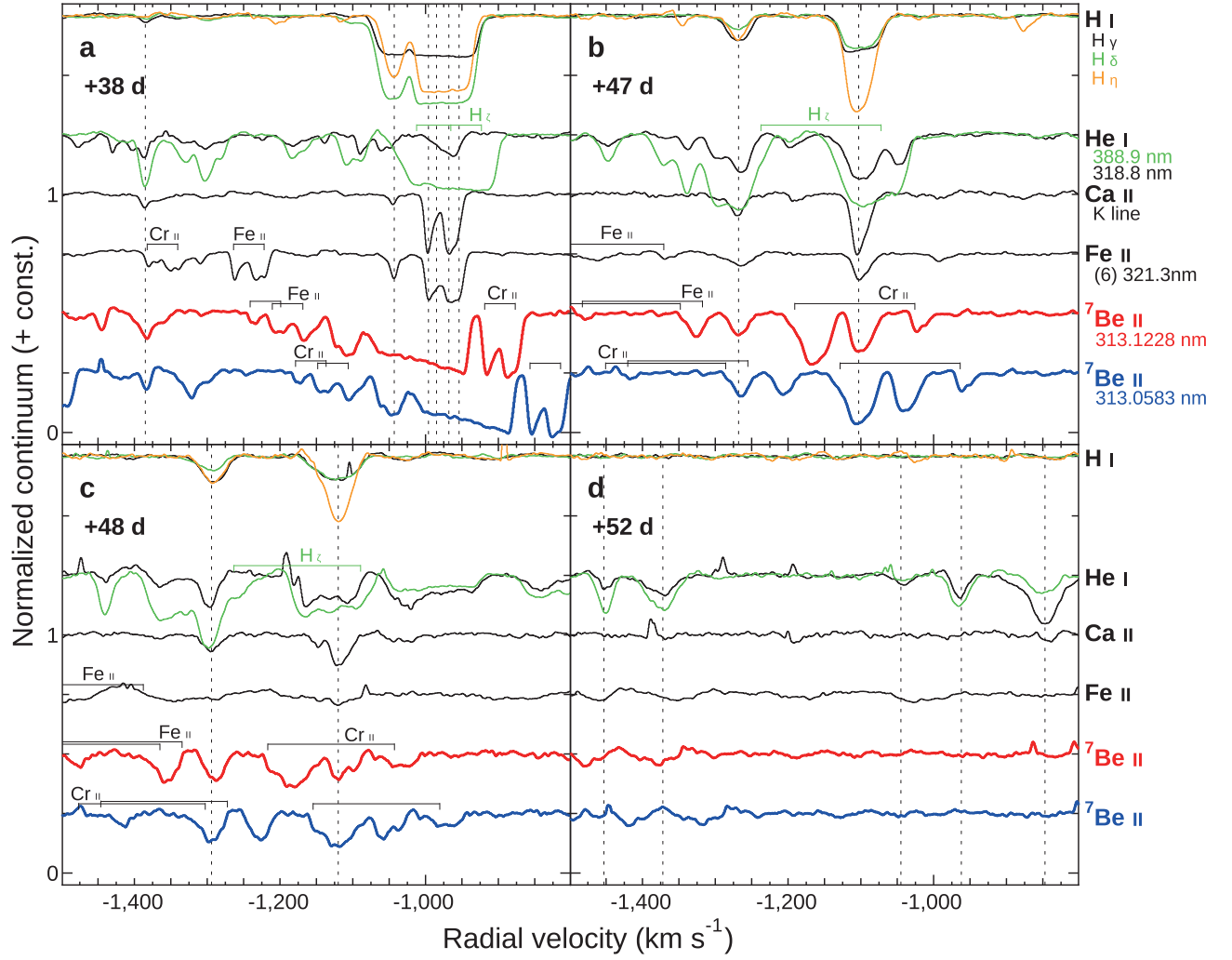


Figure 2: **Time variations of the blue-shifted absorption line systems from +38 to +52 d.**

Absorption line systems originating from different species at four observing epochs are plotted on the velocity scale. All lines are normalized to the local continuum. Blue-shifted absorption components observed at each epoch are indicated by vertical dashed lines. The identified line or expected line contaminations are labeled above each lines. **a**, On +38 d, the profile of the ${}^7\text{Be II}$ doublet around $v_{\text{rad}} \sim -1,000 \text{ km s}^{-1}$ is complicated, and possibly interpreted as being saturated. **d**, On +52 d, no blue-shifted absorption can be found except for the metastable He I lines.

Methods

Discovery V339 Del (= Nova Delphini 2013) is a classical nova that was discovered as a bright 6.8 magnitude (unfiltered) source by Koichi Itagaki on 2013 August 14.584 UT and announced in American Association of Variable Star Observers (AAVSO) Alert Notice⁶. Its progenitor is estimated to be a blue star USNO B-1 1107-0509795 with $B \sim 17.20$, $R_C \sim 17.45$ on the first Palomar Sky Survey Plates (exposed on 1951 July 7), and with $B \sim 17.39$, $R_C \sim 17.74$ on the second Palomar Sky Survey plates (exposed on 1990 July 18 and September 15, respectively)³¹. No significant changes were found in its photometric behavior for at least a few years prior to the outburst³². On an unfiltered pre-discovery image obtained on 2013 August 13.998 UT, the object was still at 17.1 mag³³. This means that the object was still in quiescence until at least 14 hours before its discovery, and that it showed a very fast rise to the maximum. After 40 hours from the discovery, maximum was reached on Aug 16.25 (MJD = 56,520.25) at $V = 4.3$ (ref. 7). Then, it began a normal decline. The nova had been detected as a transient high energy gamma ray (> 100 MeV) source within ~ 10 days after the outburst³⁴. Angular sizes of the expanding shell around the nova had been monitored until $\sim +40$ d using near-infrared interferometric observations³⁵. Then, combining the expansion velocity obtained in the optical region, the distance to the nova had been derived as 4.54 ± 0.59 kiloparsecs from the Sun.

Observations and data reduction Post-outburst spectra of V339 Del were obtained using the High Dispersion Spectrograph (HDS)³⁶ of the 8.2 m Subaru Telescope at four epochs from 2013 September 23 to October 7 (+38, +47, +48, and +52 d after the maximum). According to the AAVSO light curves (see in Extended Data Fig. 1), our first observation was just before the start

of the rapid decline in optical magnitudes by dust formation³⁷. The following three were obtained during the continuous decline. We obtained spectra under 3 configurations of the spectrograph, which cover the wavelength regions from 303 to 463 nm, from 411 to 686 nm, and from 667 to 936 nm. Spectral resolving power was set to $R \simeq 90,000$ or 60,000 with $0''.4$ (0.2 mm) or $0''.6$ (0.3 mm) slit widths, respectively. The exact times and wavelength ranges of obtained spectra are summarized in Extended Data Table 1. Data reduction was carried out using the IRAF software in a standard manner. The non-linearity in the detectors are corrected by the method described in ref. 38. The wavelength calibration has been performed using a Th-Ar comparison spectrum and the typical residual in wavelength calibration is $\lesssim 10^{-4}$ nm (~ 0.1 km s⁻¹) for each spectrograph configuration. The typical systemic variance of the spectrograph is $\lesssim 10^{-4}$ nm per an hour. We also examined the accuracy of radial velocity determination in our measurement using the identified iron-group transitions in 315–351 nm. For the spectrum obtained at +38d, the velocity of the strongest component in the absorption line system was -996.1 ± 0.7 km s⁻¹ determined by Gaussian fittings. In total, we concluded that the residual in our velocity scale determination was $\sim \pm 1$ km s⁻¹. Spectrophotometric calibration was performed using the spectrum of BD+28° 4211 (ref. 39) obtained nearly at the same altitude of the nova on the same nights. All spectra were converted to the heliocentric scale. Correction for interstellar extinction has not been applied. The average signal-to-noise ratio in the spectra obtained at four epochs is ~ 140 at ~ 312 nm, where we found the ⁷Be lines.

Highly blue-shifted absorption line system The spectra of V339 Del exhibit a series of broad Fe II emission lines, which indicate that the object is a typical Fe II type nova¹². Since no strong

emission originating from Ne is found in the spectrum even in +52 d, the WD in the system is supposed to be a CO-WD¹³.

Extended Data Fig. 2-a displays the radial velocity profiles of three Fe II belonging to multiplet number⁴⁰ (42) in the spectrum of +38 d. The absorption line system on +38 d clearly consists of five components at $v_{\text{rad}} = -954, -968, -985, -996$, and $-1,043 \text{ km s}^{-1}$ as indicated by the dashed lines in Extended Data Fig. 2-b. Similarly, blue-shifted absorption components are found in Balmer lines (Extended Data Fig. 2-c) and also in other permitted lines (Ca II H and K, He I at 587.6 nm). In the near UV range, numerous absorption lines in the complex continuum are identified as the transitions of singly ionized iron-group species. Most of them belong to the absorption line systems found in the visual region (Extended Data Fig. 3). We applied a Doppler correction using the radial velocity of the strongest blue-shifted absorption line in the system to identify sources of transitions (see in Extended Data Fig. 3-b). We use the velocities for Doppler corrections as $v_{+38} = -996$, $v_{+47} = -1,103$, and $v_{+48} = -1,120 \text{ km s}^{-1}$ for +38, +47, and +48 d, respectively (in Extended Data Fig. 3-b and Fig. 4-a, b, and c). All of the identified transitions originate from levels of low excitation potentials ($\lesssim 4 \text{ eV}$). The residual intensity at the bottom of these lines exceeds 75 % of the continuum, while the bottoms of some strong Fe II and Balmer lines show flat structures. These observations suggest that the saturated absorption lines are created by clouds of absorbing gas, which cover the continuum emitting region by only about 25 %.

Very similar short-lived blue-shifted metallic absorption systems (Transient Heavy Element Absorption; THEA) have been reported in post-outburst spectra of several classical novae⁸. Especially, great majority of novae show strong blue-shifted ($400\text{--}1,000 \text{ km s}^{-1}$) multiple absorption

components in the Na I D doublet in days following their outbursts. In the very slow nova V1280 Sco, multiple high-velocity (700–900 km s^{−1}) absorption components have been found in the Na I D doublet even 800 days after its maximum⁹. Although no absorption components of the Na I D are found at all epochs of our observations of V339 Del, other characteristics of the absorption line systems found in V339 Del are quite similar to those of the THEAs in other novae. They are (a) highly blue-shifted ($\sim 1,000$ km s^{−1}), (b) divided into several velocity components, (c) time variable in their shapes and velocities, and (d) short-lived (2–8 weeks).

Contamination to the ⁷Be II doublet We carefully inspected possible contaminations of absorption lines originating from other species to the ⁷Be II lines consulting the atomic line database⁴¹. Extended Data Fig. 4 displays the spectra in the vicinity of the ⁷Be II doublet obtained at four epochs of our observations.

On the spectrum obtained at +47 d, there are no candidates to contaminate the −1,103 or the −1,268 km s^{−1} components of ⁷Be II at 313.1228 nm, which we use in our ⁷Be abundance estimation (see in Extended Data Fig. 4-b).

At this epoch, the other line of the ⁷Be doublet at 313.0583 nm may be contaminated by some lines originating from iron-group species. We estimate that the −1,268 km s^{−1} component of Cr II (5) at 313.205 nm ($\log gf = +0.079$) may contaminate to the −1,103 km s^{−1} component of this ⁷Be II line. The influence of this contamination can be evaluated adopting the line strength ratio between the pair of velocity components of Cr II (5) at 312.497 nm ($\log gf = +0.018$) to that of Cr II (5) at 313.205 nm. It is quite small compared with the strength of the ⁷Be II line ($\lesssim 5\%$).

Concerning the $-1,268 \text{ km s}^{-1}$ component of this $^7\text{Be II}$ line, we conclude that the weak lines of Fe II (96) at 312.901 nm ($\log gf = -2.70$) and Cr II (5) at 312.869 nm ($\log gf = -0.32$) do not contaminate severely. This is because similar weak lines of Fe II (82) at 313.536 nm ($\log gf = -1.13$) and Cr II (5) at 313.668 nm ($\log gf = -0.25$) had completely disappeared until $+47 \text{ d}$. We can neglect the contamination from the V II (1) line at 313.0257 nm ($\log gf = -0.29$), because the other V II (1) line at 312.621 nm ($\log gf = -0.27$) is not detected on our spectra.

^7Be abundance estimation We empirically estimate the abundance of ^7Be in the absorbing gas by comparing the equivalent widths of the $^7\text{Be II}$ line with those of the Ca II K line that are the similar transitions on the atomic energy level diagrams. We assume that the covering factor of the absorbing gas cloud to the background illuminating source has no wavelength dependence. This method could be a simple and robust approach to estimate the abundance ratio independent of ejecta models for nova explosions. The estimate, however, includes some uncertainties. One is the difference in the ionization potentials between Be (the first and second ionization potentials; $I_1 = 9.32$, $I_2 = 18.21 \text{ eV}$) and Ca ($I_1 = 6.11$, $I_2 = 11.87 \text{ eV}$)¹⁴ that could result in a difference of ionization states between Be and Ca. However, all of iron-peak elements (Ti to Fe) found in the absorption line systems, which have intermediate ionization potentials ($I_1 = 6.75\text{--}7.90$, $I_2 = 13.58\text{--}18.12 \text{ eV}$) between those of Be and Ca, are observed only in singly ionized states, suggesting that dominant fractions of Be and Ca are in the singly ionized states, too. In the obtained spectra, we could not find any resonance lines of Sr II or Ba II , which correspond to those of Be II and Ca II . The Sr/Ca and the Ba/Ca number ratios would be quite small, as seen in the solar abundance ($\ll 10^{-3}$). Another uncertainty is the $X(\text{Ca})$ in the absorption line system. Our

assumption that the absorbing gas has the solar $X(\text{Ca})$ would not be far from the reality, because the theoretical analysis predicts no overabundance of elements with the mass number >30 in ejecta of CO novae²¹. We remark that our ${}^7\text{Be}$ abundance estimation is carried out using the data obtained at +47 d, which is close to the half-life of ${}^7\text{Be}$ (53.22 days). Therefore, the abundance of the freshly produced ${}^7\text{Li}$ in this nova explosion could be ~ 2 times higher than the $X({}^7\text{Be})$ on +47 d.

31. Munari, U. & Henden, A. Photometry of the progenitor of Nova Del 2013 (V339 Del) and calibration of a deep BVRI photometric comparison sequence. *Inform. Bull. Variable Stars* **6087**, 1 (2013).
32. Deacon, N. R. *et al.* Pre-outburst observations of Nova Del 2013 from Pan-STARRS 1. *Astron. Astrophys.* **563**, A129 (2014).
33. Denisenko, D. *et al.* V339 Delphini = Nova Delphini 2013 = Pnv J20233073+2046041. *IAUCirc.* No. **9258**, 2 (2013).
34. The Fermi-LAT Collaboration. Fermi establishes classical novae as a distinct class of gamma-ray sources. *Science* **345**, 554–558 (2014).
35. Schaefer, G. H. *et al.* The expanding fireball of Nova Delphini 2013. *Nature* **515**, 234–236 (2014).
36. Noguchi, K. *et al.* High Dispersion Spectrograph (HDS) for the Subaru Telescope. *Publ. Astron. Soc. Jpn* **54**, 855–864 (2002).

37. Shenavrin, V. I., Taranova, O. G. & Tatarnikov, A. M. Dust formation in Nova Del 2013. *Astron. Telegr.* **5431**, 1 (2013).
38. Tajitsu, A., Aoki, W., Kawanomoto, S. & Narita, N. Nonlinearity in the Detector used in the Subaru Telescope High Dispersion Spectrograph. *Publ. Natl. Astron. Obs. Jpn* **13**, 1–8 (2010).
39. Massey, P., Strobel, K., Barnes, J. V. & Anderson, E. Spectrophotometric standards. *Astrophys. J.* **328**, 315–333 (1988).
40. Moore, C. E. *A Multiplet Table of Astrophysical Interest: NBS Technical Note No. 36, Reprinted Version of the 1945 edition* (US Department of Commerce, 1959).
41. Kurucz, R. & Bell, B. Atomic Line Data. *Atomic Line Data (R.L. Kurucz and B. Bell) Kurucz CD-ROM No. 23. Cambridge, Mass.: Smithsonian Astrophysical Observatory, 1995.* **23** (1995).

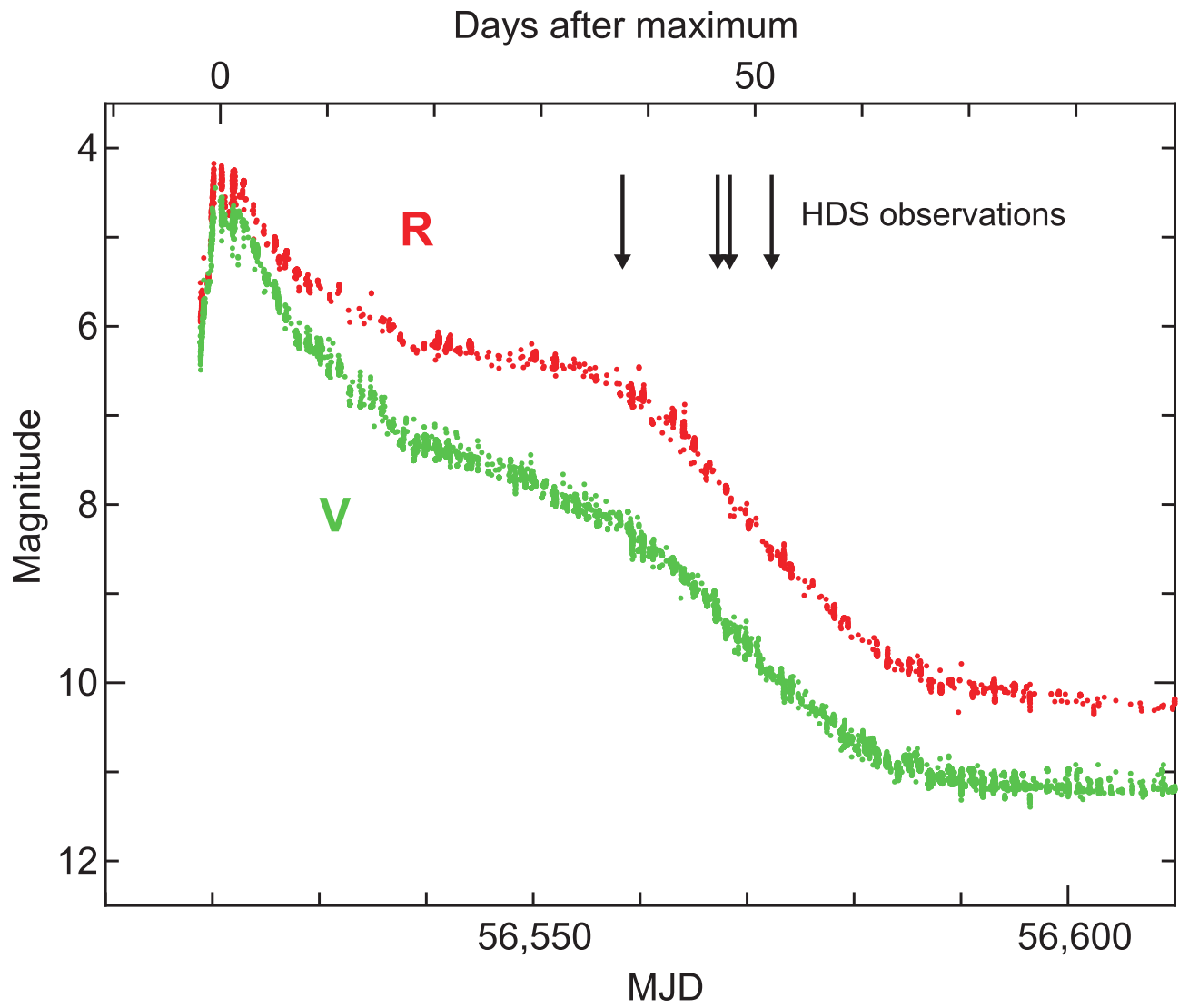
Extended Data Table 1: **Journal of HDS observations of V339 Del**

Extended Data Fig. 1: **Optical light curves of V339 Del.** V (green) and R (red) magnitudes are taken from the AAVSO database. The epochs of our HDS observations are indicated by arrows.

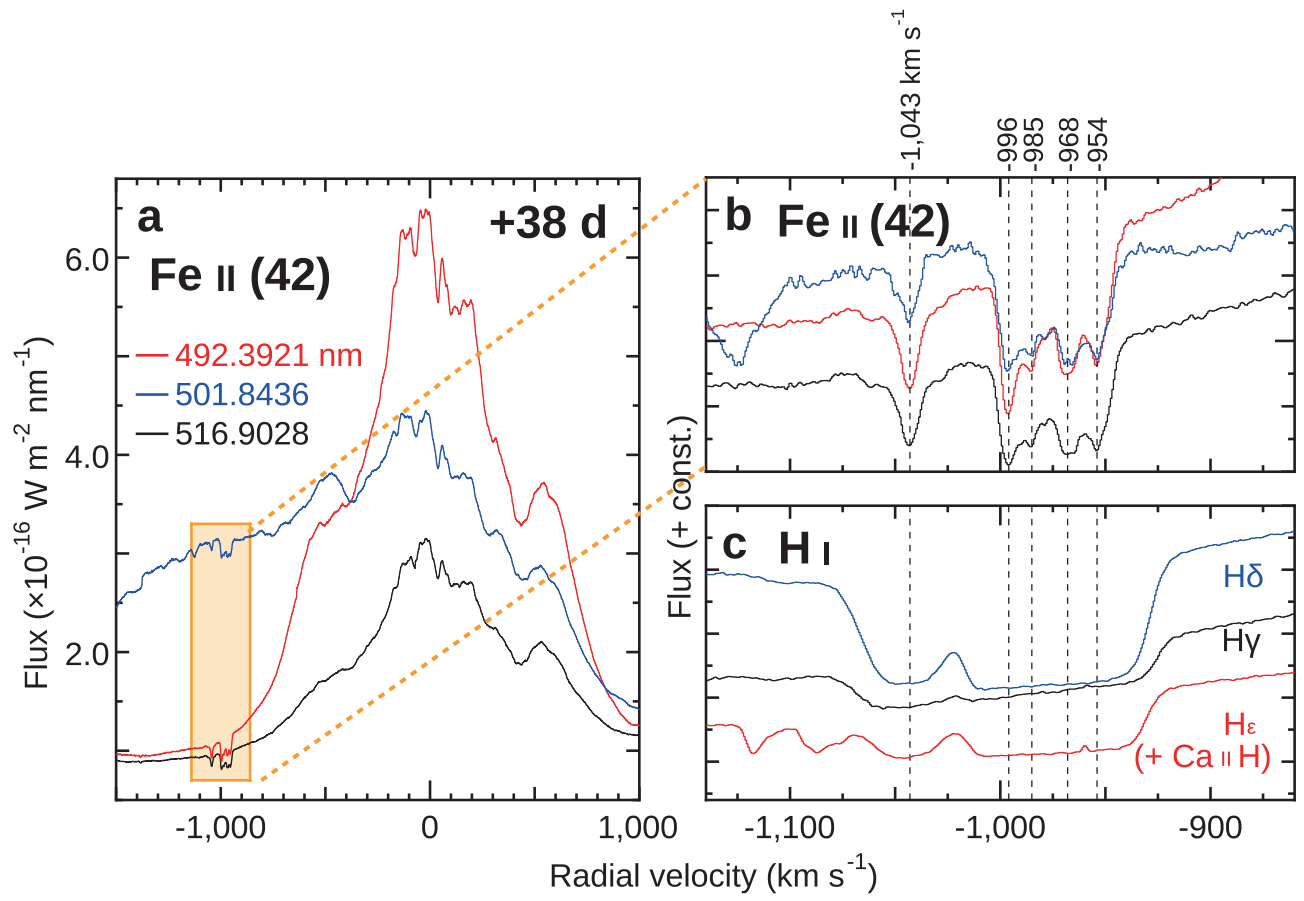
Extended Data Fig. 2: **Optical spectrum of V339 Del obtained at +38 d.** Panel **a** shows the radial velocity plots of three Fe II emission lines belonging to the same multiplet number³⁰ (42). In addition to the similarity of their broad emission profiles, all lines have common blue-shifted absorption line features around $v_{\text{rad}} \sim -1,000 \text{ km s}^{-1}$. Panel **b** shows the enlarged view of the absorption line features in panel **a**. Dips of individual absorption line are indicated with dashed lines. **c**, The absorption line systems in H I Balmer lines drawn on the same velocity scale as in panel **b**.

Extended Data Fig. 3: **Near UV spectrum of V339 Del obtained at +38 d.** Panel **a** shows the overall view of the spectrum from 308 to 350 nm. Identified Fe II emission lines are indicated with red ticks at the bottom. The identified absorption line systems originating from iron-group ions – Fe II (red), Ti II (blue), Cr II (green), Mn II, Ni II, and V II (black) – are indicated by ticks at the top. Panel **b** shows a sample of the absorption line identification. The results of our identification are displayed along the spectrum. **c**, Same as Extended Data Fig. 2-**b**, but for two lines (Ti II and Cr II) highlighted in panel **b** are plotted on the velocity scale.

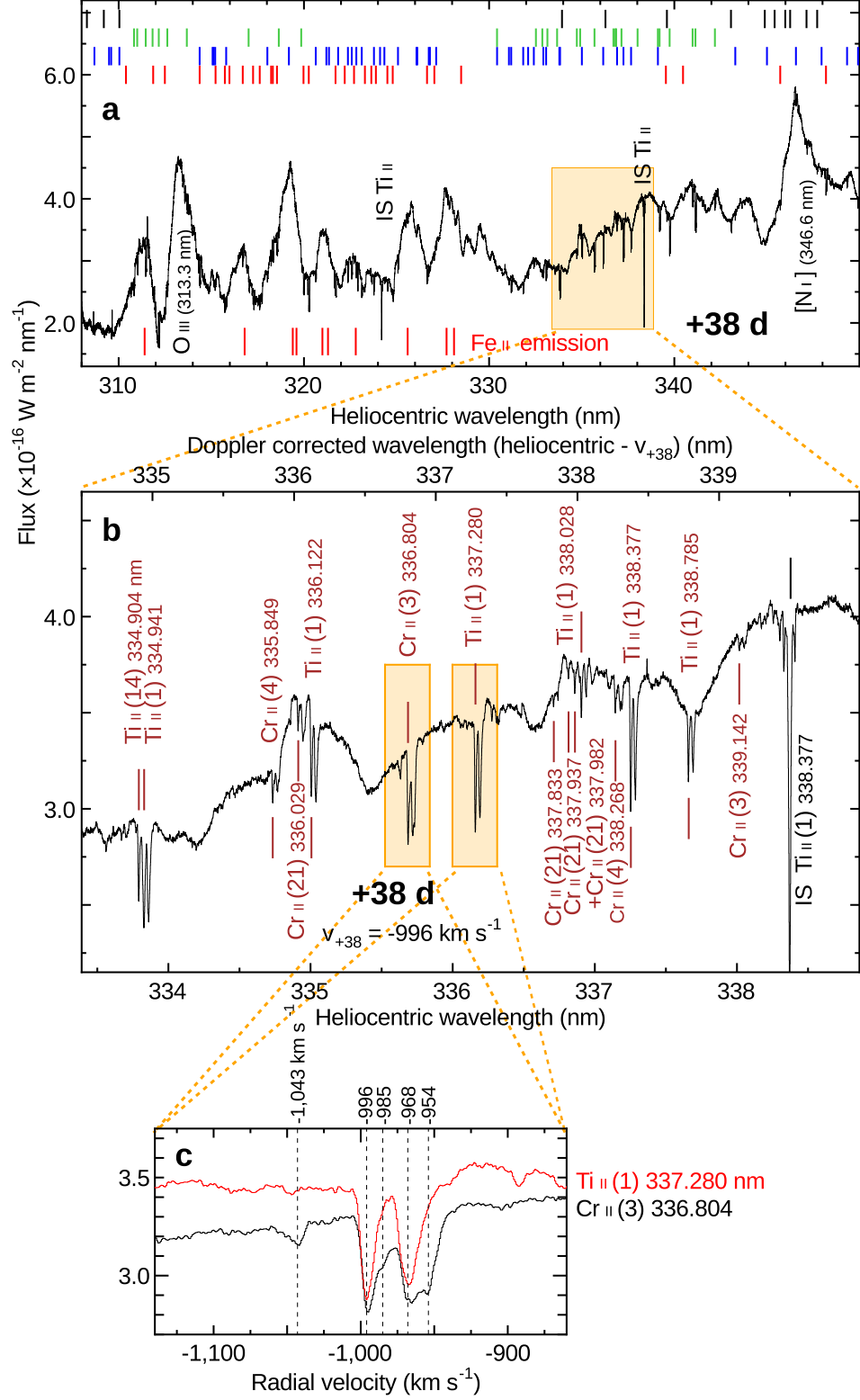
Extended Data Fig. 4: **Spectra in the vicinity of the Be II doublet from +38 to +52 d.** **a – c**, The horizontal scale is displayed with the heliocentric (bottom) and the Doppler corrected wavelengths (top). The Doppler corrections are applied using $v_{\text{days}} = v_{+38}$, v_{+47} , and v_{+48} for panels **a**, **b**, and **c**, respectively. The local continuums fitted with high order (10–20) spline functions are over-plotted with green lines. The positions of the strongest ($v_{\text{rad}} = v_{\text{days}}$) and the second strongest components of the absorption line system are indicated by colored long and short lines connected by horizontal bars. **d**, Since no apparent absorption lines are found in +52 d, the spectrum is applied a Doppler correction using v_{+48} .



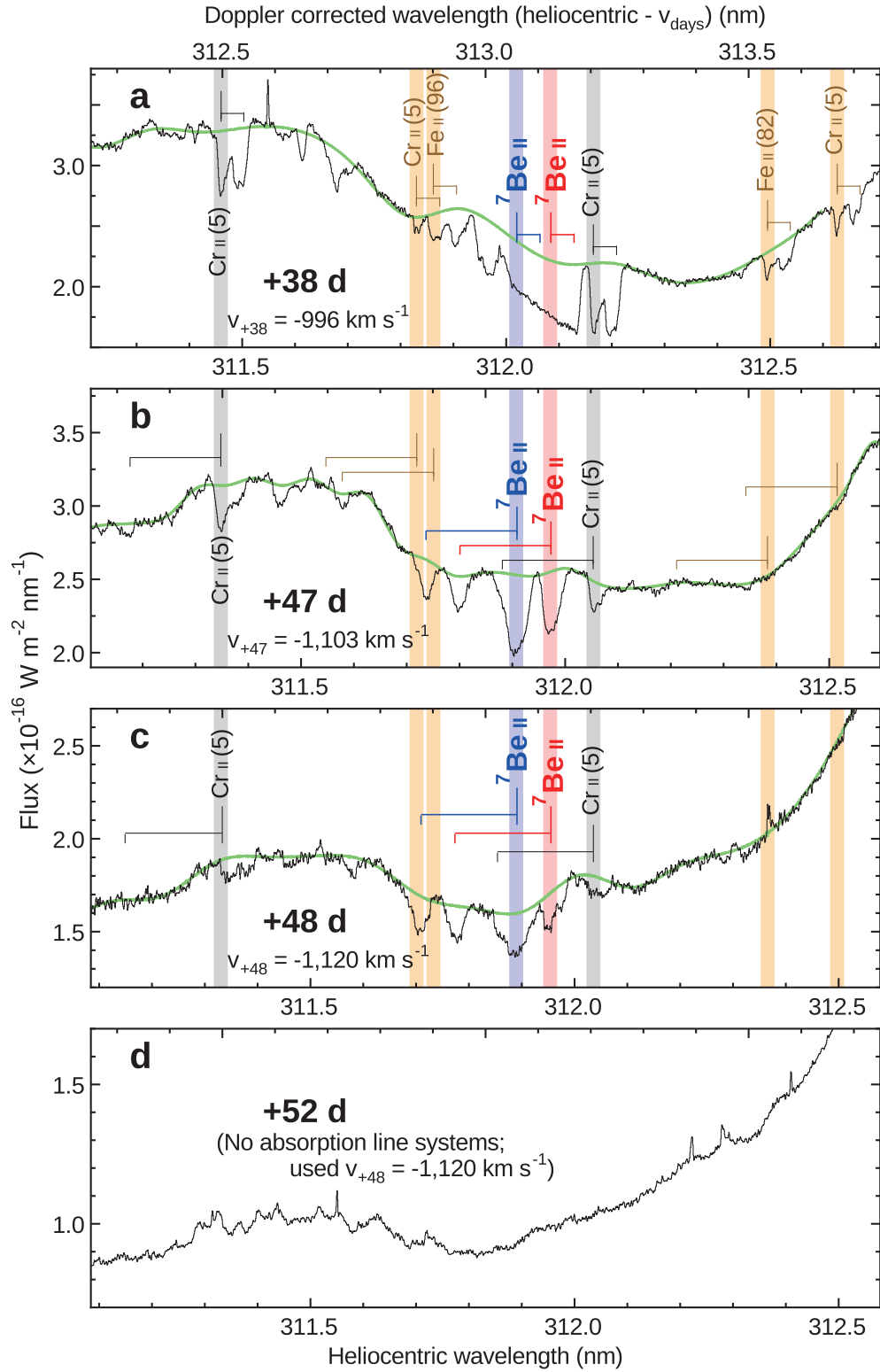
Extended Data Fig. 1: **Optical light curves of V339 Del.**



Extended Data Fig. 2: **Optical spectrum of V339 Del obtained at +38 d.**



Extended Data Fig. 3: Near UV spectrum of V339 Del obtained at +38 d.



Extended Data Fig. 4: Spectra in the vicinity of the Be II doublet from +38 to +52 d.

Extended Data Table 1: **Journal of HDS observations of V339 Del**

Date 2013	UT* (h m)	MJD		Exposure (s)	Range (nm)	Resolution
Sep 23	6 16	56,558.261	(+38 d) [†]	720	411-686	90,000
	8 12	56,558.342		900	667-936	90,000
	10 07	56,558.423		3,000	303-463	90,000
Oct 02	5 02	56,567.210	(+47 d) [†]	3,000	303-463	60,000
	6 29	56,567.271		600	411-686	90,000
	7 18	56,567.305		900	667-936	90,000
Oct 03	9 21	56,568.390	(+48 d) [†]	3,000	303-463	60,000
Oct 07	5 05	56,572.212	(+52 d) [†]	4,800	303-463	60,000
	7 47	56,572.324		960	411-686	90,000
	8 17	56,572.346		1,500	667-936	90,000

* UT is the universal time at the start of an exposure.

[†]Days after the optical (V) maximum (MJD = 56,520.25).